Kissing and nanotunneling mediate intermitochondrial communication in the heart

Xiaohu Huang[a], Lei Sun[b], Shuangxi Ji[c], Ting Zhao[a], Wanrui Zhang[a], Jiejia Xu[a], Jue Zhang[c], Yanru Wang[a], Xianhua Wang[a], Clara Franzini-Armstrong[d,1], Ming Zheng[a,e,1], and Heping Cheng[a]

[a]State Key Laboratory of Biomembrane and Membrane Biotechnology, Institute of Molecular Medicine, Peking-Tsinghua Center for Life Sciences, and [c]College of Engineering, Peking University, Beijing 100871, China; [b]Center for Biological Imaging, Institute of Biophysics, Chinese Academy of Sciences, Beijing 100101, China; [d]Department of Cell and Developmental Biology, University of Pennsylvania Medical School, Philadelphia, PA 19104-6058; and [e]Department of Physiology, Health Science Center, Peking University, Beijing 100083, China

Contributed by Clara Franzini-Armstrong, January 15, 2013 (sent for review November 12, 2012)

Mitochondria in many types of cells are dynamically interconnected through constant fusion and fission, allowing for exchange of mitochondrial contents and repair of damaged mitochondria. However, constrained by the myofibril lattice, the ∼6,000 mitochondria in the adult mammalian cardiomyocyte display little motility, and it is unclear how, if at all, they communicate with each other. By means of target-expressing photoactivatable green fluorescent protein (PAGFP) in the mitochondrial matrix or on the outer mitochondrial membrane, we demonstrated that the local PAGFP signal propagated over the entire population of mitochondria in cardiomyocytes on a time scale of ∼10 h. Two elemental steps of intermitochondrial communications were manifested as either a sudden PAGFP transfer between a pair of adjacent mitochondria (i.e., "kissing") or a dynamic nanotubular tunnel (i.e., "nanotunneling") between nonadjacent mitochondria. The average content transfer index (fractional exchange) was around 0.5; the rate of kissing was 1‰ s^{-1} per mitochondrial pair, and that of nanotunneling was about 14 times smaller. Electron microscopy revealed extensive intimate contacts between adjacent mitochondria and elongated nanotubular protrusions, providing a structural basis for the kissing and nanotunneling, respectively. We propose that, through kissing and nanotunneling, the otherwise static mitochondria in a cardiomyocyte form one dynamically continuous network to share content and transfer signals.

mitochondrial dynamics | nanotubule

In most cells, mitochondria are highly dynamic organelles that constantly undergo shape changes through fusion and fission. This results in a form of communication that allows for the exchange and distribution of soluble and membranous components, including metabolic intermediates, signaling messengers, proteins, lipids, and mitochondrial DNAs, and provides a mechanism for repairing damaged mitochondria and maintaining a healthy mitochondrial population (1–3). Disorders of mitochondrial fusion and fission have been associated with developmental defects, neurodegenerative diseases, and cardiovascular diseases (4–7).

In adult mammalian cardiomyocytes, mitochondria occupy ∼40% of the cell volume and are rigidly organized between bundles of myofilaments (interfibrillar mitochondria), under the sarcolemma (subsarcolemmal mitochondria), and around the nucleus (perinuclear mitochondria). This arrangement and the apparent lack of motility, a prerequisite for mitochondrial fusion in other types of cells, raise the question of whether mitochondria in adult cardiomyocyte communicate with each other dynamically. Mitochondrial dynamics in cardiac cell lines or neonatal cardiomyocytes (8) do not provide a direct answer to this question because mitochondria in these cells are not constrained strictly. Limited studies with adult cardiomyocytes have been inconclusive and even controversial. Whereas low-amplitude and high-frequency mitochondrial fluctuations have been visualized and quantified in living adult cardiomyocytes, no mitochondrial fusion and fission was detected (9). In isolated adult rat heart challenged by short periods of hypoxia (10) and in cardiomyopathy patients (11), elongated mitochondria ranging from three to seven sarcomeres in length have been visualized, whereas in cardiomyocytes from heart failure patients and rat models, increased amounts of small and fragmented mitochondria were detected (12), indicating the occurrence of mitochondrial fusion and fission or other as-yet-unknown type of dynamic regulation. Pharmacological treatment with a mitochondrial fission protein the dynamin-related protein Drp1 inhibitor increases the proportion of elongated mitochondria in rat cardiomyocytes and protects the heart against ischemia–reperfusion injury (13), further suggesting a crucial role of mitochondrial dynamics in cardiac function.

Using mitochondria-targeted expression of photoactivatable green fluorescent protein (PAGFP) in conjunction with confocal microscopy, we investigated mitochondrial dynamics in living adult rat cardiomyocytes over extended periods of time. We found that mitochondria communicate with each other, with the elemental steps manifesting as discrete, sudden content transfer events between adjacent ("kissing") or long-range mitochondrial pairs ("nanotunneling"). As a result, the entire population of mitochondria forms one dynamically continuous network, such that the membranous or matrix contents of individual mitochondria mix and exchange over the whole cardiomyocyte on a timescale of ∼10 h.

Results

Mitochondria Are Dynamically Interconnected in Adult Cardiomyocytes. In adult rat cardiomyocytes stained with the mitochondrial membrane potential indicator tetramethyl rhodamine methyl ester (TMRM), optically resolved interfibrillar mitochondria were mostly rod-shaped and each was confined to a single sarcomere of ∼2 μm in length (Fig. S1*A*) (8). However, unlike mitochondria in many other cell lines, time-lapse imaging revealed little motility over as long as 2 h (Fig. S1 *A* and *B*), indicating that cardiac intermitochondrial communication, if any, must be achieved by means other than the "collision, fusion, and fission" mechanism common to other cell types.

To investigate the intermitochondrial communication in cardiomyocytes, we expressed a photoactivatable green fluorescent protein in the mitochondrial matrix (mtPAGFP) and detected a 40-fold increase in local mtPAGFP fluorescence upon photoactivation (illuminated by 405-nm laser for 60 ms) (Fig. 1*A*, *Upper*). Photoactivated mtPAGFP appeared to be sharply confined to the portion of the cell that underwent laser illumination over a few minutes. In sharp contrast, photoactivated cytosolic PAGFP

Author contributions: X.H., M.Z., and H.C. designed research; X.H., L.S., S.J., T.Z., W.Z., J.X., Y.W., X.W., and C.F.-A. performed research; X.H., S.J., J.X., J.Z., C.F.-A., M.Z., and H.C. analyzed data; and X.H., M.Z., and H.C. wrote the paper.

The authors declare no conflict of interest.

[1]To whom correspondence may be addressed. E-mail: zhengm@pku.edu.cn or armstroc@mail.med.upenn.edu.

This article contains supporting information online at www.pnas.org/lookup/suppl/doi:10.1073/pnas.1300741110/-/DCSupplemental.

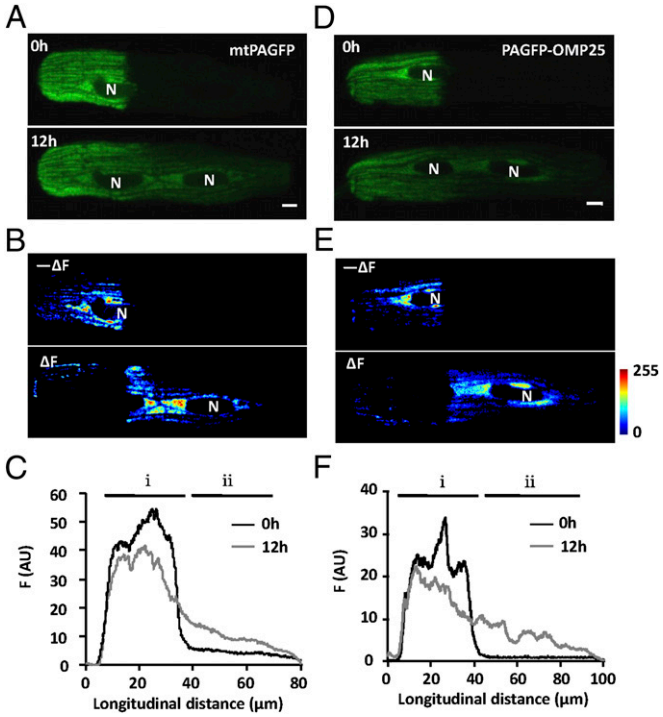

Fig. 1. Intermitochondrial communication in adult rat cardiomyocytes. (*A* and *D*) Confocal images of cardiomyocytes transfected with adeno-mtPAFGP (*A*) or adeno-PAGFP-OMP25 (*D*), immediately after photoactivation (*Upper*) or 12 h later (*Lower*). (Scale bars: 5 μm.) (*B* and *E*) Regional loss (−△F) and gain of fluorescence (△F) at 12 h after photoactivation. N, nucleus. (*C* and *F*) Distribution of PAGFP fluorescence along the cell length at indicated time points. i, photoactivated area; ii, nonactivated area.

diffused rapidly, leading to a uniform cell-wide increase of fluorescence intensity within ∼30 s (Fig. S2). To our surprise, when we reexamined the photoactivated cardiomyocytes in culture 12 h after photoactivation, we found that the mtPAGFP signal had spread over the entire cell (Fig. 1*A*, *Lower*): the nonactivated region was brighter (△F) at the expense of fluorescence loss from the photoactivated region (−△F) (Fig. 1*B*), whereas the total mtPAGFP signal was essentially unchanged. The spatial profile of mtPAGFP intensity (averaged across the cell width) at 12 h revealed a clear redistribution down a left-to-right decreasing concentration gradient (Fig. 1*C*). Thus, we concluded that dynamic exchange of mitochondrial matrix content does occur in adult cardiomyocytes in the absence of mitochondrial motility.

To determine whether mitochondrial membrane components exchange as well, we opted to use PAGFP-OMP25 (14) in which PAGFP was fused with the membrane-targeting sequence mitochondrial outer membrane protein 25 (OMP25). Upon photoactivation of PAGFP-OMP25, we detected a sharply confined initial PAGFP-OMP25 signal that showed no immediate bulk propagation (Fig. 1*D*, *Upper*). At 12 h, however, maps of local gain (△F) and loss (−△F) of fluorescence, as well as the spatial profile plot, showed clear propagation of PAGFP-OMP25 from the photoactivated region toward the nonactivated portion of the cell (Fig. 1 *D*–*F*). Taken together, these data suggest that, despite the intersarcomere physical discontinuity and the lack of bulk movement, all mitochondria in an adult cardiomyocyte form one dynamically continuous network, exchanging both matrix and membranous components over a timescale of ∼10 h.

Mitochondrial Kissing in Cardiomyocytes. In principle, cardiac mitochondrial communication may occur via a slow but continuous diffusion process; alternatively, it may comprise intermittent, discrete elemental steps analogous to fusion and fission. To discriminate between these possibilities, a large number of cells expressing mtPAGFP were monitored at a finer time resolution (one frame per 3 s) to catch any rare events, and simultaneous TMRM staining was used to optically locate individual mitochondria. After photoactivating a 24-μm^2 rectangular area and surveying for 10 min in 94 cells, we successfully recorded 77 events of sudden intermitochondrial content transfer between two neighboring mitochondria, termed mitochondrial "kissing." The frequency of occurrence of kissing was estimated to be 0.23‰ s^{-1} (assuming six mitochondria flanked a photoactivated region), and all these kissing events occurred within the same longitudinal mitochondrial bundle. Time course plots showed that a sudden decrease of fluorescence in a photoactivated mitochondrion occurred concomitantly with an abrupt increase of fluorescence in a neighboring nonactivated mitochondrion (Fig. 2 *A* and *B*, and Movie S1), with their sum of fluorescence unchanged. The stepwise transition was completed within 49 ± 3.4 s (n = 24) for mtPAGFP, whereas conventional mitochondrial fusion has a briefer transition time (14). Spatiotemporal analysis showed that content exchange was restricted to the pair of kissing mitochondria (mito-1 and mito-2) because no change in the mtPAGFP signal was evident in their immediate neighbors (mito-3, mito-4, and mito-5) (Fig. 2*D*). Importantly, differing from conventional mitochondrial fusion, kissing was not associated with any detectable movement of the mitochondrial pair (Fig. 2*E*) and

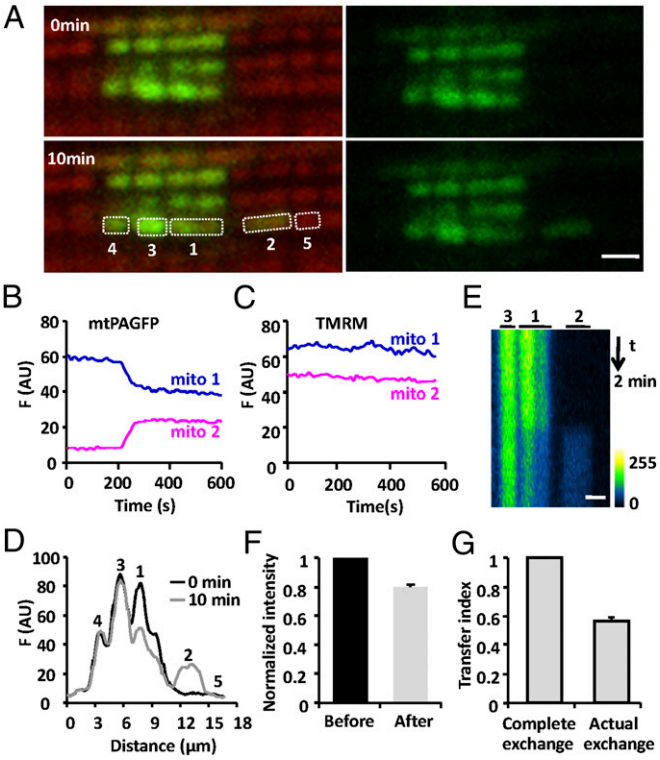

Fig. 2. Kissing between a pair of adjacent mitochondria. (*A*) Confocal images of interfibrillar mitochondria in cardiomyocytes expressing mtPAGFP and stained with TMRM, at indicated time points after photoactivation. (Scale bar: 2 μm.) (*B*) Time courses of mtPAGFP fluorescence in adjacent mitochondria, mito-1 and mito-2. (*C*) As in *B*, for TMRM fluorescence. (*D*) Spatial profiles showing the mtPAGFP fluorescence intensity along the mitochondrial bundle immediately or 10 min after photoactivation. (*E*) Space–time visualization of a mitochondrial kissing event. Time runs from top to bottom and mitochondrial location is shown horizontally. (*F*) Normalized mtPAGFP fluorescence intensity in donor mitochondria before and after kissing. (*G*) Mitochondrial transfer index.

simultaneous TMRM staining showed no detectable changes in the mitochondrial membrane potential either (Fig. 2*C*).

If the content exchange was at equilibrium, no fluorescence intensity difference between donor (F1) and acceptor (F2) mitochondria would be expected after the transition. However, the donor was often still brighter than the acceptor even after the transfer (Fig. 2*B*), indicating that the content exchange was incomplete. We defined the transfer index as $\delta = 1 - D2/D1$, where D1 and D2 refer to the fluorescence difference (F1 − F2) before and after the transfer, and found that the transfer index varied from 0.35 to 1, with an average value of 0.57 ($n = 27$), far from complete mixing ($\delta = 1$) (Fig. 2*G*). Our data suggested that kissing is too brief to allow for equilibrium between kissing mitochondria. In this scenario, kissing reflects a transient physical connectivity of otherwise segregated mitochondria and the aforementioned transition time provides a good estimate of the kiss duration.

Mitochondrion-to-Mitochondrion Nanotunneling. To our further surprise, we found that intermitochondrial communication occurred between pairs of well-separated mitochondria in a saltatory fashion, bypassing their intermediate neighbors. In Fig. 3*A* and Movie S2, sequential confocal images showed a sudden increase of the mtPAGFP signal in a remote mitochondrion (mito-5) about 8 μm away from a photoactivated mitochondrion (mito-1) in an adjacent interfibrillar mitochondrial bundle. With enhanced image contrast, we showed that a slender thin structure emerged and protruded from mito-1, moved across three intermediate mitochondria, mito-2, mito-3, and mito-4, and connected with mito-5, which showed an abruptly augmenting mtPAGFP signal (Fig. 3*B*) before this structure disappeared soon after the content transfer. We named this phenomenon "nanotunneling." It is noteworthy that the synchronous changes of the mtPAGFP signal were confined to mito-1 and mito-5 without affecting the fluorescence intensity in the three intermediate mitochondria (Fig. 3 *C* and *D*). A total of 21 nanotunneling events was observed in 298 cells over a 10-min time window, suggesting its incidence is about 14 times less frequent than that of mitochondrial kissing. Together, our findings suggest that kissing and nanotunneling constitute elemental steps of mitochondrial dynamics in adult cardiomyocytes.

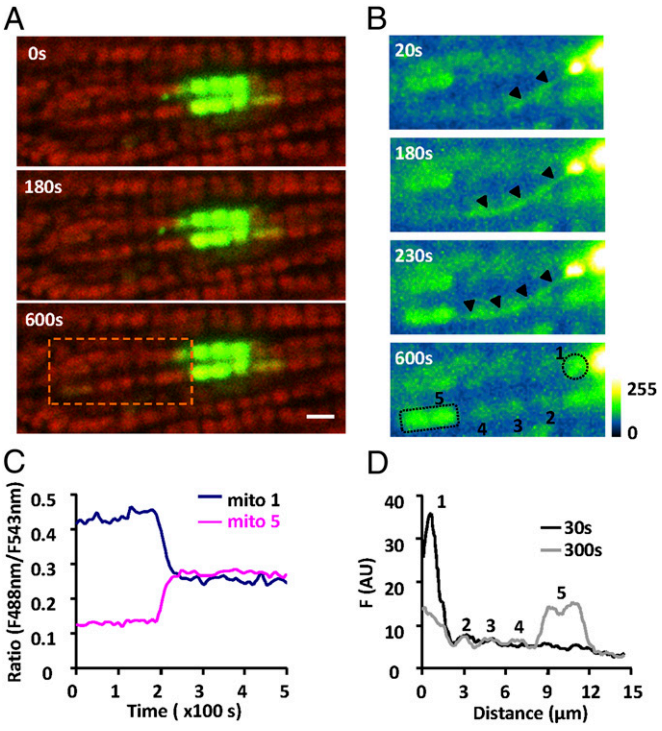

Fig. 3. Nanotunneling between two distant mitochondria. (*A*) Confocal images show the overlapped mtPAGFP (green) and TMRM signals (red) at indicated time points after photoactivation. (Scale bar: 2 μm.) (*B*) Enlarged views of the area outlined by the rectangle in *A* with enhanced mtPAGFP signal. Note the emergence and disappearance of a tubular mitochondrial structure (arrowheads) that mediated the remote transfer of mtPAGFP between two well-separated mitochondria without affecting the intermediate ones. (*C*) Time courses of the ratio of the mtPAGFP/TMRM fluorescence (F488/F543) for mito-1 and mito-5 marked in *A*. (*D*) Distribution of mtPAGFP fluorescence in mitochondria as indicated in *B* at 30 and 300 s after photoactivation.

Ultrastructural Basis for Kissing and Nanotunneling. To elucidate the basis of mitochondrial kissing and nanotunneling, we performed transmission electron microscopy (TEM) and found two directly relevant structural details. The first was the presence of very intimate contacts ("kissing junctions") between adjacent mitochondria both at their ends and where they abutted laterally. Most mitochondria, even where restrained between the myofibrils, had several opportunities for such contacts (Fig. 4*A*). Each contact extended over up to several hundred nanometers and within it the outer membranes had repeated sites where the two membranes seemed to actually touch with no detectable intervening space. Such contacts are highly probable candidates for the exchange of either outer membrane components or matrix proteins. Similar kissing junctions were recently described in skeletal muscle (15).

The second detail was a form of mitochondrial structure that seemed to be directly relevant to nanotunneling. As shown in Fig. 4*B*, a double-membrane, tubular structure extended from mitochondrion i, bypassed three mitochondria in the same bundle, and was finally connected with mitochondrion ii. These mitochondrial nanotubules were delimited by a double membrane and displayed diameters ranging from 90 to 210 nm. Nanotubules connecting two adjacent mitochondria in adult cardiomyocytes were rarely detected (Fig. 4*C*), as may be expected because the probability of following one nanotubule for its entire course in a thin section was low. Most frequently, we observed nanotubules connected with only one mitochondrion and possibly projecting from it, giving rise to a "tadpole" appearance (Fig. 4*D*), and also apparently disconnected nanotubules (Table S1). Because the tubules were often seen to extend over several sarcomeres, they were the most likely basis for the nanotunneling events that we observed, but it was not clear whether the nanotubules established a direct continuity between the matrices of two mitochondria or whether they connected to the exchange partner via the equivalent of a kissing junction.

Because the experiments were performed in isolated cardiac myocytes that were maintained for several days in culture, and because this is likely to encourage some loosening of the myofibrils and liberation of mitochondria, we investigated whether the presence of kissing junctions and nanotubules is dependent on the time spent in culture. An examination of freshly fixed hearts and of isolated myocytes between 0 and 3 d in culture revealed that kissing junctions were very numerous and nanotubules were also present in the in situ heart. The frequency of nanotubules was slightly higher in cells that were kept in culture for 3 d relative to freshly plated cells, but the increase was very small (Table S1). This means that the structures necessary for kissing and nanotunneling communication are present in the normal intact heart.

Quantitative Modeling of Mitochondrial Kissing and Nanotunneling. At first glance, the kissing and nanotunneling events appeared to be relatively infrequent, occurring once every ~1 h for a mitochondrial pair (~5,000 events per h in a cardiomyocyte). So, we investigated whether these elemental events fully account for the cell-wide propagation of a local signal through the mitochondrial population. We devised a mathematical model for computer simulation and compared it with the spatiotemporal profiles of mtPAGFP spread. In the computer model, 50 units of mitochondria, each 2 μm long,

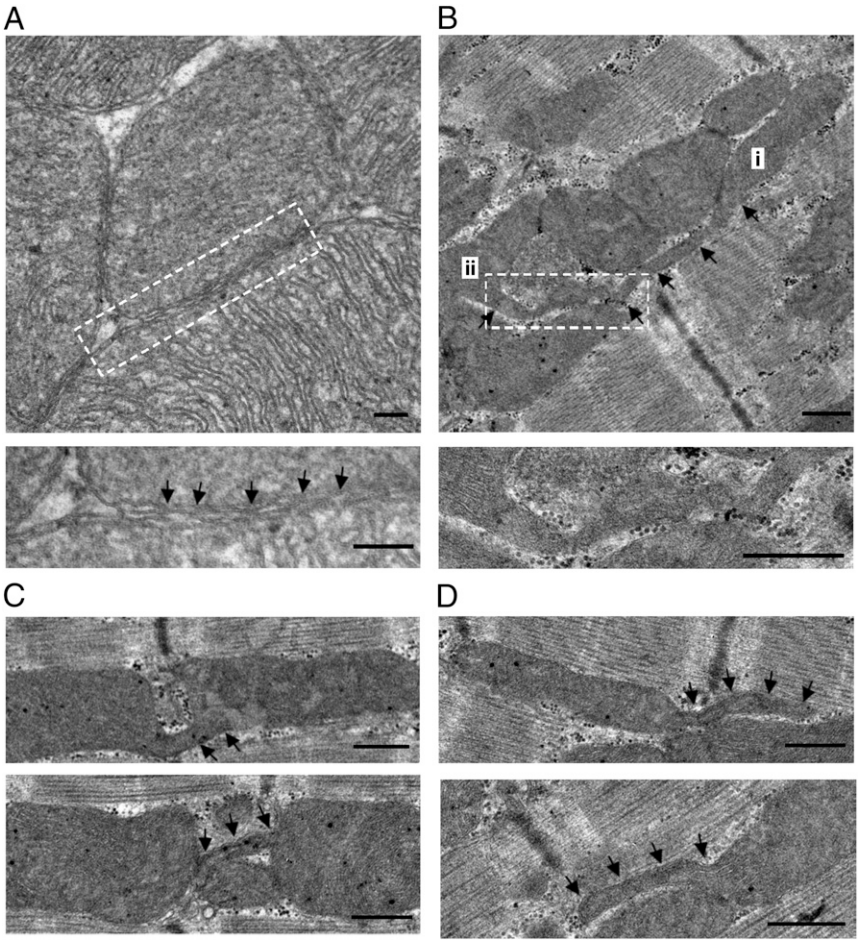

Fig. 4. Ultrastructure of cardiac mitochondria. (*A*) TEM data showing intimate kissing junctions between adjacent mitochondria. In the enlarged detail, the outer membranes of the two closely apposed mitochondria establish close contacts at repeated sites (arrows). (*B*) A nanotubular structure bridging long-distance mitochondria shown by i and ii. (*C*) Nanotubules connecting adjacent mitochondrial pairs. Note that the tubular structure in the upper panel traverses the gap at the Z-line to connect the mitochondrial pair. (*D*) Nanotubules extending (traced by arrows) from mitochondria in the interfibrillar area. (Scale bar: 500 nm.)

were positioned linearly in tandem (Fig. 5*C*). Kissing (between two adjacent mitochondria) and nanotunneling (between a mitochondrion and its second or third neighbor on either side) occurred at different rates (p1, p2) but with a constant δ. We experimentally measured the mtPAGFP signal along mitochondrial bundles at 2, 4, and 6 h after photoactivation of a 10.6 μm × 5.9 μm rectangular area (Fig. 5 *A* and *B*). The model parameters were then obtained by nonlinear least-square fitting of the Monte Carlo-simulated results to the experimental data, giving p1 a value of 1‰ s^{-1}; p2, 0.05‰ s^{-1}; and δ, 0.33. Remarkably, this simple model closely reproduced the mtPAGFP spatial profiles at all three time points after photoactivation (Fig. 5*D*). In the simulation, there were totals of 1,048 kissing and 52 nanotunneling events in 6 h among the 50-mitochondrion bundle, with no fluorescence change when kissing and nanotunneling pairs contained no or equal photoactivated mtPAGFP. Taken together, these experimental and modeling results strongly suggest that kissing and nanotunneling are forms of mitochondrial dynamics that may quantitatively account for the kinetics of local intermitochondrial communication in adult cardiomyocytes.

Communication Among Perinuclear Mitochondria. The data in Fig. 1 showed that mtPAGFP and PAGFP-OMP25 propagated farther along the mitochondrial bundle connecting two nuclei of binucleate cardiomyocytes, suggesting a more efficient communication among perinuclear as well as internuclear mitochondria. Morphologically, more round mitochondria are densely packed in the perinuclear areas and along the internuclear mitochondrial band (8, 16). We thus measured the propagation rate of mitochondrial content in these areas. Compared with interfibrillar mitochondria, both matrix mtPAGFP and outer membrane PAGFP-OMP25 showed a faster propagation rate in perinuclear mitochondria: the farthest front of the PAGFP signal 2 h after local photoactivation spread about 19 μm in the perinuclear area, and 6.5 μm in the interfibrillar area (Fig. 6*A*). Mitochondrial kissing was also detected among irregularly organized perinuclear mitochondria (Fig. 6 *B* and *C*), without motion and collision of the kissing mitochondrial pair. In electron micrographs (Fig. 6 *D* and *E*), we also documented more frequent nanotubules extending from round mitochondria (i.e., tadpole-shaped mitochondria), as if they were the physical conduit underlying mitochondrial content transfer. Together, our data suggest that the irregularly organized perinuclear mitochondria have more active dynamics than the strictly organized interfibrillar mitochondria.

In a subset of cells (~30%), photoactivation from one side of a nucleus led to a rapid (<2 min), gradual (no stepwise change) increase of fluorescence signal of all of the apparently segregated mitochondria encompassing the nucleus (~12-μm long axis, 5-μm short axis) (Fig. S3 *A* and *B*). This strongly suggests that perinuclear mitochondria sometimes form a single physically interconnected 3D network. Indeed, we observed synchronous mitochondrial "flashes" in the perinuclear mitochondrial network in adult cardiomyocytes expressing the superoxide biosensor mt-cpYFP (Fig. S3*E*). The flashes initiated uniformly in the highly extended perinuclear mitochondrial network, rose to a peak amplitude at about the same time, and then dissipated with similar kinetics (Fig. S3*E*). Flash events that partially enveloped the nucleus were also observed (Fig. S3*F*). Likewise, synchronous perinuclear mitochondrial membrane potential oscillation was also detected with TMRM (Fig. S3 *C* and *D*). This suggests that mitochondria in these

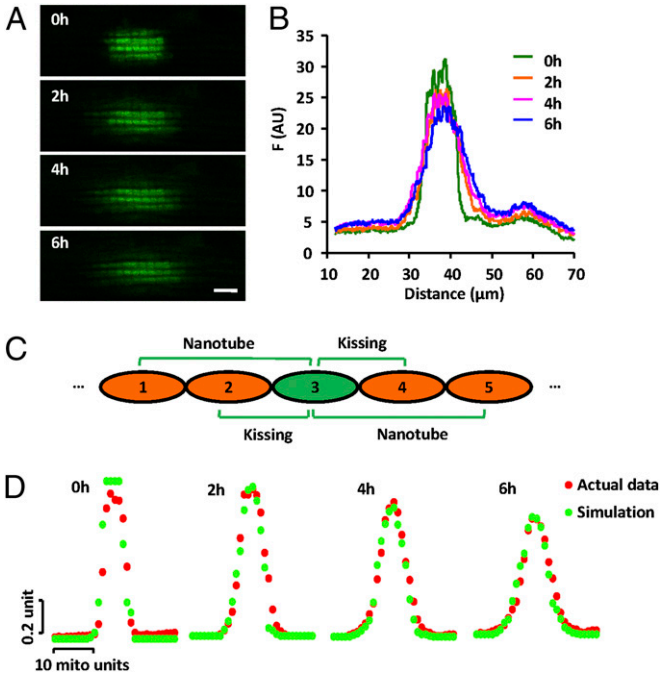

Fig. 5. Model simulation of mitochondrial communication. (*A*) Confocal images of the mtPAFGP signal at indicated time points after photoactivation of a 10.6 μm × 5.9 μm rectangular region. (Scale bar: 5 μm.) (*B*) Spatial profiles of mtPAFGP distribution corresponding to *A*. (*C*) A model of dynamic content transfer in a linear mitochondrial bundle (*Materials and Methods*). (*D*) Monte Carlo simulations at 0 h (after 50 kissing and 2 nanotunneling events), 2, 4, and 6 h (with 1,048 kissing and 52 nanotunneling events), overlaid with experimentally measured fluorescence distributions.

regions may be interconnected to form large reticular functional networks. The more active mitochondrial dynamics as well as the higher interconnectivity of perinuclear and internuclear mitochondria plays an important role in promoting content exchange over the entire mitochondrial population (Fig. 1).

Discussion

In the present study, we have demonstrated two forms of dynamic mitochondrial communication in adult cardiomyocytes—kissing between adjacent mitochondria, and nanotunneling for a mitochondrion to reach a partner over a long range. Differing from the prevalent mitochondrial fusion model in which mitochondrial motility is a prerequisite (17–19), these types of intermitochondrial communication involve structurally restricted, motionless mitochondria in cardiomyocytes. Moreover, we uncovered several prominent features of these modes of intermitochondrial communication. First of all, the transfer of membranous and matrix contents does not occur as simple diffusion through a preconnected reticular mitochondrial network. Rather, it is dynamic, manifesting as intermittent, sudden, and brief (<1 min) content transfer between two discrete mitochondria (with exceptions in the perinuclear population of mitochondria). By direct quantification and by parameter fitting the experimental data to a simple mathematic model, we estimated the rate of occurrence of kissing and nanotunneling to be 0.23–1.0‰, and the transfer index, 0.3–0.6. The latter indicates only a partial mix of the contents of the mitochondrial pair. Importantly, ultrastructural analysis revealed kissing junctions between adjacent mitochondria, as well as double-membrane nanotubules (90–210 nm in diameter) extending from mitochondria to physically connect with neighboring mitochondria or remote partners. Furthermore, time-lapse confocal imaging, together with the observation of incomplete content mixing, provides evidence for dynamic intermitochondrial connectivity. Through kissing and nanotunneling, the population of ~6,000 stationary mitochondria is dynamically connected into one continuous functional network, where a local matrix and membranous content traverses the 120-μm length of a typical cardiomyocyte over the timescales of hours and days.

Interestingly, we found remarkably enhanced intermitochondrial communication among the perinuclear and internuclear populations compared with interfibrillar mitochondria. The average transfer distance at 2 h after photoactivation was threefold greater. Consistent with this, TEM data showed densely packed mitochondria, more frequently with tadpole shapes and nanotubular projections in this special region. In addition, perinuclear mitochondria appear to form a functionally interconnected network on some occasions, evidenced by synchronous membrane potential oscillation and mitochondrial flash production that engulf the entire nucleus. It is also tempting to speculate that the dynamic perinuclear mitochondrial network is involved in mitochondria-to-nucleus signal transduction and coordination. Furthermore, our preliminary observations found dynamic, long and thin nanotubule-like structures in cultured neonatal cardiomyocytes and in HeLa cells (Fig. S4 *A* and *B*), suggesting that nanotunneling coexists with conventional mitochondrial fusion. Taken together, mitochondrial nanotunneling is likely an intrinsic

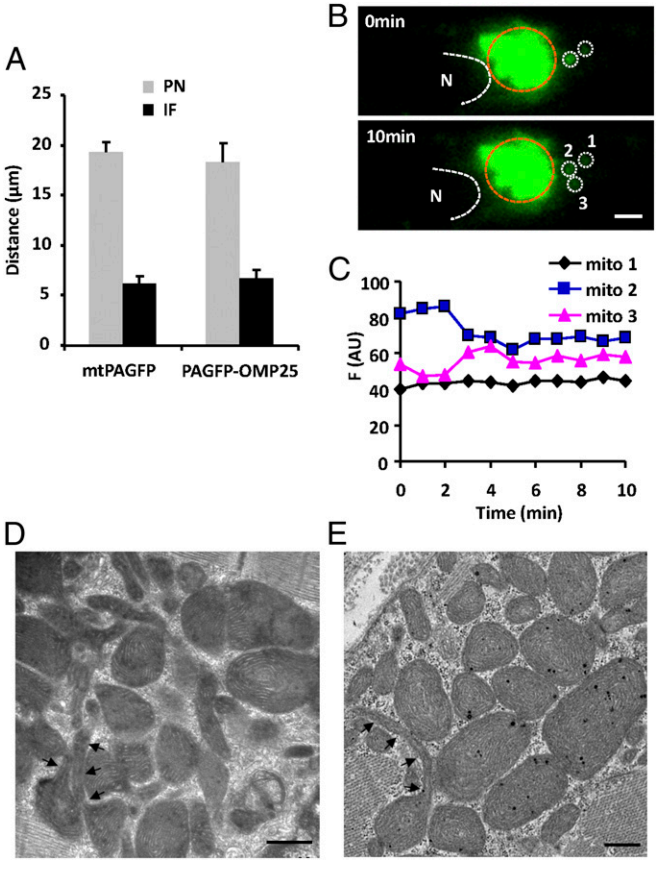

Fig. 6. Perinuclear mitochondrial communication. (*A*) Average travel distance of mtPAFGP and PAGFP-OMP25 signals 2 h after photoactivation, in mitochondria in the perinuclear (PN) and interfibrillar (IF) areas. (*B*) Confocal images showing mitochondrial kissing in the PN area. Region surrounded by brown dashed line indicates photoactivated area. (Scale bar: 2 μm.) (*C*) Fluorescence intensity changes in donor (mito 2) and acceptor mitochondria (mito 3) marked in *B*. Note the lack of change in mito 1 next to the kissing pair. (*D* and *E*) Electron micrographs of perinuclear mitochondria. The arrowheads track nanotubular structures of mitochondria. (Scale bars: 500 nm.)

property common to all mitochondria, whereas its phenotypic expression and relative contribution to intermitochondrial communication may vary in a cell type-specific manner.

The questions arise whether nanotunneling is a new property acquired only in highly specialized cells (e.g., heart cells) or a property common to all mitochondria that is best manifested in cardiomyocytes where mitochondrial fusion is ineffective due to lack of motility. An extensive literature search revealed that nanotubules may present an efficient way for organelle-to-organelle or even cell-to-cell communication. In plant cells, nanotubular structures termed stromules bridge separate chloroplasts, mediating the communication of contents between them (20, 21); similar nanotubules called plasmodesmata build routes for the intercellular transfer of nutrients and signals (22). Likewise, in various mammalian cells, intercellular nanotubules mediate long-distance cell-to-cell communication, and enable intercellular transfer of cytoplasmic contents and even organelles (23, 24). Nanotubules connecting bacteria provide superhighways for intercellular and interspecies exchange of cellular protein and DNA (25). Notably, the mitochondrial nanotubules described in this study had diameters ranging from 90 to 210 nm, similar to those between bacteria (50–130 nm) and mammalian cells (50–200 nm) (23, 25). These observations raise the possibility that nanotunneling is an ancient but conserved property that is still used by the symbiotic mitochondria and chloroplasts (26), as well as single-cell organisms, and cells in higher plants and animals.

A number of questions remain to be answered by future mechanistic investigations. It would be of interest to determine the exact molecular mechanisms underlying the formation of the kissing contact and the nanotubule, and whether they are different from or similar to those involved in mitochondrial fusion and fission. Moreover, although nanotubules can form dynamically and disappear after the content transfer (Fig. 3*B* and Fig. S4), we do not know whether all kissing and nanotubule contacts seen in the TEM (Figs. 4 and 6 *D* and *E* and Table S1) are static or dynamic structures; and, if they were static, what gating mechanism is responsible for the control of transient content transfer.

Recent studies have shown that normal mitochondrial dynamics are required to maintain the collective health and homogeneity among the mitochondrial population (1, 5, 27). As shown by us and others, defects of cardiac mitochondrial morphology are associated with a variety of heart diseases (11, 12, 28, 29), and in vivo treatment with a pharmacological inhibitor of the mitochondrial fission protein Drp1 has been suggested to provide cardioprotection against ischemia–reperfusion injury (13). Our preliminary data showed impaired mitochondrial communication in cardiomyocytes from spontaneously hypertensive rats (Fig. S5 *A–D*), a well-established model for hypertrophic heart disease. The concurrent enhancement of mtDNA damage, as reflected by a decrease in the proportion of integrated mtDNA to nuclear DNA (Fig. S5*E*), is consistent with a crucial role of mitochondrial dynamics in the maintenance of mtDNA integrity.

In summary, we have provided functional and structural evidence for kissing and nanotunneling as mechanisms allowing for slow but robust communication among immobile mitochondria in adult cardiomyocytes. With kissing and nanotunneling as the elemental steps, the entire mitochondrial population of ~6,000 units is dynamically interconnected to form one continuous mitochondrial network. Hampering such intermitochondrial communication and the unity of the network may be associated with mitochondrial dysfunction in cardiovascular diseases. The idea that nanotunneling serves as a fundamental mechanism that participates universally in organelle-to-organelle and even cell-to-cell communication (organism-to-organism for bacteria) and the underlying molecular mechanisms merit future investigation.

Materials and Methods

All animal experiments were carried out in accordance with the protocols approved by the Institutional Animal Care and Use Committee of Peking University accredited by Association for Assessment and Accreditation of Laboratory Animal Care International. Adenovirus containing mtPAGFP or PAGFP-OMP25 gene was used to infect adult rat cardiomyocytes. Detailed methods of cardiomyocyte isolation and culture, confocal microscopic and TEM analyses, simulation model, mitochondrial DNA analyses, and statistics are described in *SI Materials and Methods*.

ACKNOWLEDGMENTS. We thank Dr. Mariusz Karbowski for providing mtPAGFP plasmid, Dr. David C. Chan for providing PAGFP-OMP25 plasmid, Dr. Yan Zhang for valuable discussion, and Dr. Iain C. Bruce for editing the manuscript. This work was supported by 973 Program Grants 2013CB531203 and 2011CB809102; National Science Foundation of China Grants 30971062, 31130067, and 31221002; and National Institutes of Health Grant R01 HL 48093 (to C.F.-A.).

1. Chan DC (2006) Mitochondria: Dynamic organelles in disease, aging, and development. *Cell* 125(7):1241–1252.
2. Westermann B (2010) Mitochondrial fusion and fission in cell life and death. *Nat Rev Mol Cell Biol* 11(12):872–884.
3. Chen H, et al. (2010) Mitochondrial fusion is required for mtDNA stability in skeletal muscle and tolerance of mtDNA mutations. *Cell* 141(2):280–289.
4. Chen H, et al. (2003) Mitofusins Mfn1 and Mfn2 coordinately regulate mitochondrial fusion and are essential for embryonic development. *J Cell Biol* 160(2):189–200.
5. Chen H, Chan DC (2009) Mitochondrial dynamics—fusion, fission, movement, and mitophagy—in neurodegenerative diseases. *Hum Mol Genet* 18(R2):R169–R176.
6. Chen KH, et al. (2004) Dysregulation of HSG triggers vascular proliferative disorders. *Nat Cell Biol* 6(9):872–883.
7. Ishihara N, et al. (2009) Mitochondrial fission factor Drp1 is essential for embryonic development and synapse formation in mice. *Nat Cell Biol* 11(8):958–966.
8. Hom J, Sheu SS (2009) Morphological dynamics of mitochondria—a special emphasis on cardiac muscle cells. *J Mol Cell Cardiol* 46(6):811–820.
9. Beraud N, et al. (2009) Mitochondrial dynamics in heart cells: Very low amplitude high frequency fluctuations in adult cardiomyocytes and flow motion in non beating Hl-1 cells. *J Bioenerg Biomembr* 41(2):195–214.
10. Sun CN, Dhalla NS, Olson RE (1969) Formation of gigantic mitochondria in hypoxic isolated perfused rat hearts. *Experientia* 25(7):763–764.
11. Kanzaki Y, et al. (2010) Giant mitochondria in the myocardium of a patient with mitochondrial cardiomyopathy: Transmission and 3-dimensional scanning electron microscopy. *Circulation* 121(6):831–832.
12. Chen L, Gong Q, Stice JP, Knowlton AA (2009) Mitochondrial OPA1, apoptosis, and heart failure. *Cardiovasc Res* 84(1):91–99.
13. Ong SB, et al. (2010) Inhibiting mitochondrial fission protects the heart against ischemia/reperfusion injury. *Circulation* 121(18):2012–2022.
14. Song Z, Ghochani M, McCaffery JM, Frey TG, Chan DC (2009) Mitofusins and OPA1 mediate sequential steps in mitochondrial membrane fusion. *Mol Biol Cell* 20(15):3525–3532.
15. Picard M, White K, Turnbull DM (2013) Mitochondrial morphology, topology and membrane interactions in skeletal muscle: A quantitative three-dimensional electron microscopy study. *J Appl Physiol* 114(2):161–171.
16. Shimada T, Horita K, Murakami M, Ogura R (1984) Morphological studies of different mitochondrial populations in monkey myocardial cells. *Cell Tissue Res* 238(3):577–582.
17. Okamoto K, Shaw JM (2005) Mitochondrial morphology and dynamics in yeast and multicellular eukaryotes. *Annu Rev Genet* 39:503–536.
18. Chan DC (2006) Mitochondrial fusion and fission in mammals. *Annu Rev Cell Dev Biol* 22:79–99.
19. Liu X, Weaver D, Shirihai O, Hajnóczky G (2009) Mitochondrial "kiss-and-run": Interplay between mitochondrial motility and fusion-fission dynamics. *EMBO J* 28(20):3074–3089.
20. Kwok EY, Hanson MR (2004) Stromules and the dynamic nature of plastid morphology. *J Microsc* 214(Pt 2):124–137.
21. Natesan SK, Sullivan JA, Gray JC (2005) Stromules: A characteristic cell-specific feature of plastid morphology. *J Exp Bot* 56(413):787–797.
22. Lucas WJ, Ham BK, Kim JY (2009) Plasmodesmata—bridging the gap between neighboring plant cells. *Trends Cell Biol* 19(10):495–503.
23. Rustom A, Saffrich R, Markovic I, Walther P, Gerdes HH (2004) Nanotubular highways for intercellular organelle transport. *Science* 303(5660):1007–1010.
24. Wang Y, Cui J, Sun X, Zhang Y (2011) Tunneling-nanotube development in astrocytes depends on p53 activation. *Cell Death Differ* 18(4):732–742.
25. Dubey GP, Ben-Yehuda S (2011) Intercellular nanotubes mediate bacterial communication. *Cell* 144(4):590–600.
26. Margulis L (1975) Symbiotic theory of the origin of eukaryotic organelles; criteria for proof. *Symp Soc Exp Biol* (29):21–38.
27. Liesa M, Palacín M, Zorzano A (2009) Mitochondrial dynamics in mammalian health and disease. *Physiol Rev* 89(3):799–845.
28. Chen Y, Liu Y, Dorn GW, 2nd (2011) Mitochondrial fusion is essential for organelle function and cardiac homeostasis. *Circ Res* 109(12):1327–1331.
29. Zhao T, et al. (2012) Central role of mitofusin 2 in autophagosome-lysosome fusion in cardiomyocytes. *J Biol Chem* 287(28):23615–23625.